GEOPHYSICAL RESEARCH LETTERS, VOL. 37, L02203, doi:10.1029/2009GL041790, 2010

Transition from complex craters to multi-ringed basins on terrestrial planetary bodies: Scale-dependent role of the expanding melt cavity and progressive interaction with the displaced zone

J. W. Head[1]

Received 15 November 2009; revised 14 December 2009; accepted 28 December 2009; published 27 January 2010.

[1] The observed differences between complex craters and multi-ringed basins are described and a combined "transient cavity/displaced zone/melt cavity" model is explored to account for the observations. In this "nested melt-cavity model", the increasing influence of the percentage of the target undergoing impact melting at the sub-impact point with increasing size (the differential melt scaling of Cintala and Grieve [1998]) causes fundamental changes in the nature of the transient cavity, its relationship to the displaced zone, and its short-term collapse behavior. The transition from complex craters to two-ring basins involves expansion of the melting front into the displaced zone, formation of a two-component excavation cavity, and a concomitant radial expansion outward of the zone of maximum elastic rebound. The short-term modification stage is then dominated by the strength differences between the fluid melt in the inner cavity and rocks of the displaced zone; the highly shocked rocks at the outer margin of the expanded parabolic melting front rebound to form the expanded peak ring, moving upward and laterally inward, easily displacing fluid melt filling the inner depression. At larger sizes, differential melt scaling causes the peak ring diameter to expand relatively more rapidly than the basin rim, and upon collapse, the increased volume of melt ponds in the rebounded melt cavity inside the expanding peak ring. As the transient melt cavity further increases proportionally in size, it penetrates through the base of the displaced zone with significant consequences. The resulting modification stage now incorporates into the collapse process inward and upward movement along the base of the displaced zone; listric failure occurs inward into the fluid melt cavity beginning at the edge of the melt cavity and extending out along the base of the displaced zone up to the base of the rim structural uplift (at ~1.5 crater radii). This forms an additional outer ring and a resulting megaterrace, modifying the radial ejecta on the collapsed rim to form a domical facies. At multi-ring basin scales, the significantly deeper penetration that occurs in the expanding melt cavity accounts for the maximum crustal thickness decrease that occurs inside the peak ring in the final basin. Early onset and higher density of peak ring basins on Mercury is predicted by higher mean impact velocity and differential melt scaling. **Citation:** Head, J. W. (2010), Transition from complex craters to multi-ringed basins on terrestrial planetary bodies: Scale-dependent role of the expanding melt cavity and progressive interaction with the displaced zone, *Geophys. Res. Lett.*, *37*, L02203, doi:10.1029/2009GL041790.

1. Introduction

[2] The morphological transition from complex craters to two-ringed basins (peak-ring basins; PRB) and the origin of multiple rings in planetary impact basins has been of fundamental interest for decades: unknown is whether the transition and the additional rings arise from properties of the substrate, properties of the impactor, gravity-strength variation, variations in the cratering process as a function of scale, or a combination of these factors (see discussions by *Melosh* [1989] and *Spudis* [1993]). The major morphological transitions (best exemplified on the Moon and Mercury) that require explanation in any theory of basin ring formation are briefly described. A synthesis of recent impact cratering studies is then used to assess the morphology and characteristics of the transition from complex craters to multi-ringed basins and to explore a geological process model for the nature of these transitions.

2. Crater to Basin Morphologic Transitions

[3] The transition from simple bowl-shaped craters to complex craters involves the formation of wall terraces, flat floors and central peaks. The transition from complex craters to peak-ring basins involves the initial suppression and widening of the central peaks, transition through "protobasins" (central peak and peak ring [*Pike*, 1988]) and then replacement of the central peaks by the development of a ring of peaks and massifs that progressively increases in diameter as a function of crater size (the peak ring/crater diameter ratio increases with size) [*Head*, 1977; *Pike*, 1988]. With increasing size, a third ring is added to form a multi-ringed basin (MRB). Although there is debate about the position and equivalence of rings in peak ring and multi-ringed basins, analysis of the well-preserved 930 km diameter lunar Orientale basin suggests that the third ring (Cordillera) is an outer ring added to the exterior of an enlarged peak ring basin (Outer Rook approximates rim, 620 km; Inner Rook, the peak ring, 430 km) [*Head*, 1974, 1977; *Head et al.*, 1993; *Spudis*, 1993]. Also observed in Orientale is a steep-walled, flat floored inner depression ~320 km in diameter and several km deep [*Williams and Zuber*, 1998]. In addition to the rings, geological units observed in Orientale include the Hevelius Formation, radially textured material extending away from the Cordillera ring, the Montes Rook Formation, a knobby unit between the Cordillera and the Outer Rook rings, and the Maunder Formation, a corrugated and smooth plains facies found

[1]Department of Geological Sciences, Brown University, Providence, Rhode Island, USA.

0094-8276/10/2009GL041790$05.00

inside the Outer Rook ring [*Head*, 1974; *McCauley*, 1977]. Gravity data for Orientale have been interpreted to mean that the thickness of the crust changes significantly (from ~50–60 km to ~10 km) across the boundary from the Inner Rook Mountains to the inner depression [*Wieczorek et al.*, 2006].

[4] The transition from complex craters to peak-ring basins to multi-ringed basins follows generally similar morphological transitions as a function of increasing size on different planetary bodies [*Pike*, 1988; *Spudis*, 1993]; however, the onset diameters for these transitions, their detailed morphology, and the density of basins of different types, show some differences from body to body. For example, Mercury displays the highest density of PRB in the Solar System and a low onset diameter [*Wood and Head*, 1976].

[5] On the basis of these observations, the following characteristics of the complex crater to multi-ring basin transition and the nature of the rings and units in the relatively unmodified Orientale basin need to be accounted for in models of their origin: 1) CP > PB > PRB: the transition from complex central peak crater (CP) to proto-basin (PB) to PRB, the ring ratio that sets it apart from other ring relationships [*Pike*, 1988], and the different PRB onset diameter and density on Mercury and the Moon; 2) PRB > MRB: the addition of a third ring (outer?), and fourth ring (inner?); 3) Associated MRB Facies: the appearance and nature of the associated geological units as exemplified by Orientale (Hevelius, Montes Rook and Maunder Formations); 4) Gravity and Crustal Thickness: the steep gradient in decreasing crustal thickness in Orientale inside the Inner Rook Mountains. Previous hypotheses for the origin of these four main characteristics are now summarized and recent developments in impact cratering processes are applied to explore candidate explanations for the observations.

3. Previous Interpretations

[6] *Schultz* [1988] pointed out that most workers interpret the morphology of PRBs to be modified complex craters, with the inner ring as a ring of peaks and the outer ring as the crater rim crest. This configuration has been attributed to 1) a discontinuity in pre-impact crustal structure, 2) a simple progression from CP in small craters, 3) an uplifted remnant of an inflection in the excavation crater profile related to the crater formation process, 4) some unspecified process related to impact velocity, or 5) part of a continuum of morphologies reflecting the degree of gravity-induced uplift/collapse of the transient crater cavity (see details by *Schultz* [1988]).

[7] The nature of the transition from PRB to MRB has been intensely debated but on the basis of the comprehensive synthesis of observations and theories by *Spudis* [1993], the most commonly held interpretation is that the outermost Cordillera ring represents the addition of an outer ring to a two-ringed basin. The topography of the inner ring (edge of the inner depression) has been attributed to post-impact thermal subsidence related to equilibration of impact heating and uplift of geotherms [*Bratt et al.*, 1985]. *Spudis* [1993] (in his synthesis) and *Head et al.* [1993] (using Galileo multispectral data), supported and helped confirm earlier interpretations that the Hevelius Formation represented radial ejecta from Orientale, that the Maunder Formation represented facies of impact melt lying inside the Outer Rook Mountain ring, and that the Montes Rook Formation represented Orientale ejecta modified during the latter part of the basin-forming event. At the time of this synthesis [*Spudis*, 1993], the position of the rim-crest equivalent was debated (Outer Rook or inward?) due primarily to a dark ring thought to represent the presence of a pre-Orientale impact, and thus to constrain the rim to inside the Outer Rook ring. More recent data have shown that the ring is a pyroclastic annulus around a central vent [*Weitz et al.*, 1998], thus removing a major objection to the assignment of the Outer Rook as the crater rim equivalent. This observation, together with the concentration of impact melt facies (Maunder Formation) inside the Outer Rook ring, strongly supports the Outer Rook as the closest approximation to the transient cavity rim crest.

4. Developments in Studies of the Impact Cratering Process

[8] Two developments in the understanding of impact cratering processes have provided new insights into the formation of craters and basins. First, as summarized by *Melosh* [1989] and *Spudis* [1993], the realization of the importance of the "displaced zone", the area below the growing transient cavity that compresses and moves downward and radially away from the sub-impact point (Figure 1a), was a major factor in understanding the importance of the depth of excavation, the shape of the transient cavity, the nature of cavity growth and collapse, and implications for the depth of sampling. The formation of the displaced zone also explained the nature and source of the structural uplift of the crater rim (hinge-like uplift out to as much as ~1.5 of the crater radius from the rim [*Settle and Head*, 1977]). These developments resulted in a significantly better understanding of the crater and basin-forming process (see summaries by *Melosh* [1989] and *Spudis* [1993]). Remaining uncertain, however, were the processes involved in the actual formation of rings and the cause of the observed transitions.

[9] Following these fundamental syntheses, additional developments have occurred that provide new insight into impact cratering at large scales. Among the most important for understanding the complex crater to basin transition was a series of papers by R. A. F. Grieve and M. J. Cintala [*Grieve and Cintala*, 1992, 1997; *Cintala and Grieve*, 1994, 1998]. These contributions used data from hypervelocity experiments, theory, modeling and terrestrial craters to assess the role of projectile kinetic energy partitioning as a function of increasing energy and scale of the cratering event. *Grieve and Cintala* [1992] used the fact that the volume of impact melt, relative to that of the transient cavity, increases with the magnitude of the impact event to investigate the influence of this factor on the nature of terrestrial impact craters. They found that with increasing impact event size, the depth of melting approaches the depth of the transient cavity; a consequence of this trend is that the sub-impact point, destined to become the rebound-induced uplifted central structure in a complex crater, will instead be subject to shock stresses sufficient to cause melting. As the depth of melting approaches the depth attained by the

transient cavity, the floor of the transient cavity has progressively less strength, and thus central peaks will not be produced during cavity modification and uplift. *Grieve and Cintala* [1992] proposed that differential scaling between crater dimensions and melt volumes could thus be a possible mechanism for the transition from central peaks in complex craters to peak rings. *Grieve and Cintala* [1997] further pointed out that the changing ratio of peak-ring diameter to rim-crest diameter as a function of increasing size observed for the Moon [*Head*, 1977] and Mercury [*Wood and Head*, 1976] could be attributed to the relative increase in the depth and volume of melted target material in the transient cavity with increasing size of the event. *Cintala and Grieve* [1998] applied the consequences of differential scaling to lunar craters, exploring size-dependent changes in the dynamics of simple to complex crater formation, and accounting for the major observed changes in morphology, impact melt distribution, and melt purity (relative abundance of clasts).

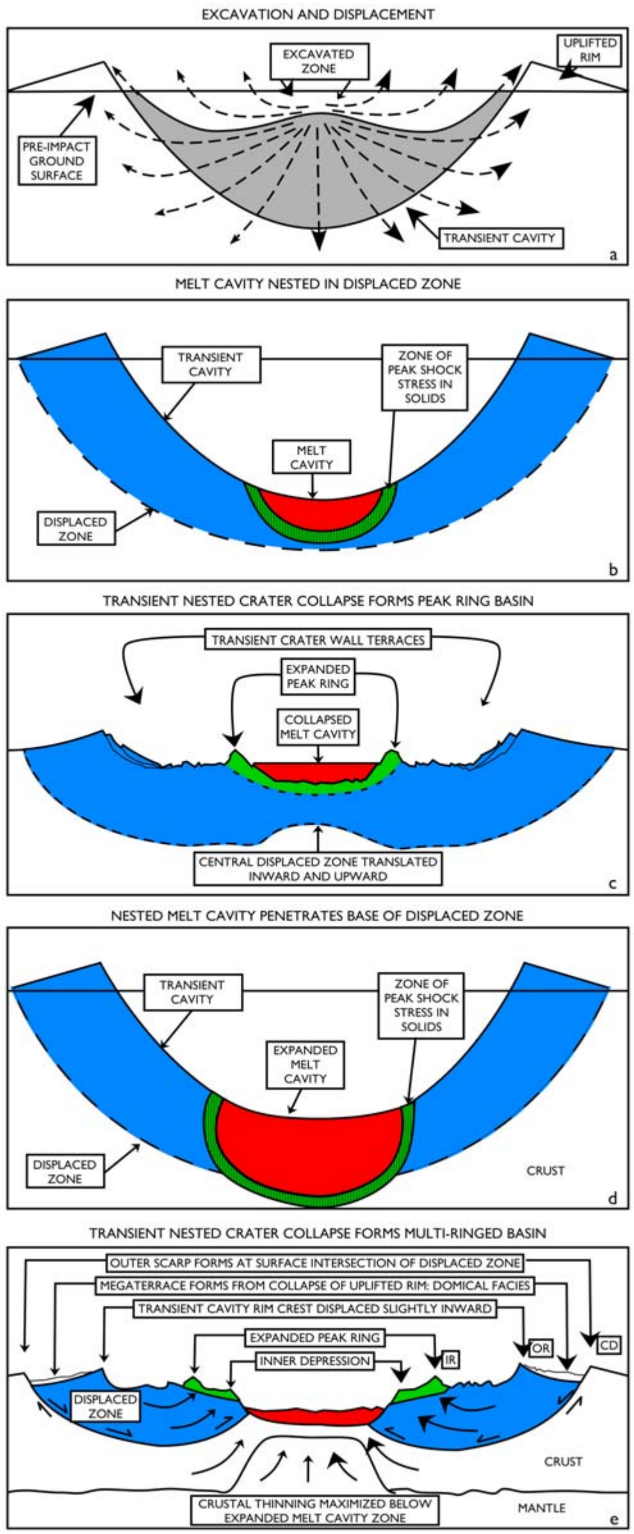

5. Application to Basin Formation

[10] Combined with the concept of the displaced zone, the Cintala and Grieve model has significant consequences and predictions for large crater and basin processes and the four major trends in the crater to basin transition outlined above. What accounts for the transition from complex crater to protobasin and to PRB? With increasing event size, proportionally more impact melt is produced and a new phase of cavity evolution emerges. The central cavity of melted material grows along the axis of penetration, becomes proportionally deeper and more voluminous, and forms a second, melt-filled crater-like feature inside the growing transient cavity (Figure 1b). The outer edge of this second ‘‘melt-cavity’’ crater is the boundary between the melted zone and the unmelted zone (the solid material that experiences peak shock stresses just short of melting). With increasing size, the depth of melting eventually overtakes the depth of excavation [*Cintala and Grieve*, 1998], penetrating down into the displaced zone, and melting deeper target material not sampled by ejecta from the transient cavity (Figure 1b).

[11] As the transient cavity rebound vectors reverse the outward paths followed during the compression phase (compare Figures 1a and 1c), the consequences are predicted to vary significantly from the case of central peak rebound in complex craters. Instead of dynamic rebound of highly shocked central peaks, the peak shock pressures in solids occur at the edge of the melt cavity [*Cintala and Grieve*, 1998], and this zone moves inward and upward to form an annulus of peaks, or a peak ring. Instead of solid rock rebound-dominated uplift and faulting (typical of complex crater central peaks), melt in the central cavity is displaced inward and upward as the cavity collapses, coating the collapsing cavity floor and ponding in the modified central crater. The differential melt-scaling model predicts that the larger the peak ring basin, the larger the

Figure 1. Nested melt-cavity model of the crater to multi-ringed basin transition. (a) Excavation and displacement in a hypervelocity impact event produces an excavated zone and a displaced zone [after *Grieve and Cintala*, 1992]. (b) Larger events will produce melt cavities nested in the displaced zone due to differential melt scaling; (c) collapse of such cavities produces peak ring basins. (d) With increasing size, the melt cavity expands and penetrates to below the base of the displaced zone (inner portions of the melt cavity area, red, are vaporized); (e) collapse of the expanded melt cavity along listric faults at the base of the displaced zone forms a multi-ring basin.

size of the peak ring should be relative to the basin diameter, a trend observed for both the Moon [*Head*, 1977] and Mercury [*Wood and Head*, 1976].

[12] The central melt cavity can be significantly deeper than the floor of the transient cavity and can thus penetrate progressively deeper into the displaced zone (Figures 1b and 1c). Melt generated in the innermost cavity is thus likely to represent melted target material originating from below the floor of the transient cavity and thus derived from greater depths than ejecta excavated from the transient cavity (compare Figures 1a and 1b). Peak rings, on the other hand, will originate from the outer margin of the melt cavity (Figures 1b and 1c), and thus will be derived from shallower crustal material than that of much of the melt cavity [*Cintala and Grieve*, 1998].

[13] What then might account for the addition of an outer and inner ring, as observed in Orientale? The onset of the main outer ring in multi-ring basins is interpreted here to be related to the same process of nested melt-cavity expansion. Outer ring formation begins to occur at larger basin diameters: As the melt cavity becomes relatively larger with increasing event size, it eventually expands downward to intersect and penetrate the base of the displaced zone. This creates a strength discontinuity at the base of the highly deformed rocks of the displaced zone and the inner, much weaker fluid-filled melt cavity wall (Figure 1d). This favors lateral movement into the cavity along the base of the displaced zone (Figure 1e). Inward and upward translation of the inner peak rings is then accompanied by deep-seated inward listric faulting along the base of the displaced zone. This listric fault propagates outward and upward to the surface, intersecting the surface at the hinge-like edge of structural uplift outside the transient cavity rim (at $\sim$1.5 crater radii). This listric fault forms an additional outer ring (an inward-facing fault scarp); collapse of the rim forms a megaterrace, modifying the innermost radial ejecta on the basin rim to the observed domical facies. Deep inside the basin, the innermost ring/depression represents the residual rebounded melt cavity. At these large multi-ring basin scales, the transient cavity, now partly defined by the extent of the melt zone, is significantly deeper in the expanding melt cavity than in the excavation zone (Figures 1d and 1e), thus accounting for the fact that the maximum decrease in crustal thickness occurs inside the peak ring in the final basin. Enhanced frictional melting [*Spray and Thompson*, 1995] may occur along the listric fault at the base of the displaced zone, with additional faulting along zones of strain localization [*Senft and Stewart*, 2009].

6. Discussion and Conclusions

[14] The "nested melt-cavity" model combines three main components of the cratering process (excavation cavity, displaced zone and melt cavity) and provides a basis for understanding the characteristics of the transition from complex craters to multi-ringed basins: Differential melt scaling [*Cintala and Grieve*, 1998] creates an increasingly larger and deeper melt cavity in the sub-impact region as a function of increasing scale (Figure 1). The progressively more significant penetration of the expanding melt cavity and its intersection with the displaced zone with increasing size leads to stepwise phases in basin collapse, from complex crater to peak ring (Figures 1b and 1c), and then from peak ring to multi-ringed basin (Figures 1d and 1e). This mechanism provides plausible explanations for the observed morphology, morphometry, facies and crustal thickness trends. The unusual characteristics of peak-ring basins on Mercury (lower transition diameter from complex crater to peak-ring basin and larger population density) can also be accounted for in this model by the higher mean impact velocity in Mercury's circum-solar environment: impactors creating complex craters on other planetary bodies are accelerated by the Sun's gravitational field to higher impact velocities at Mercury's orbit so that their resulting impact energy is sufficient to induce melting deep enough to create a peak-ring basin. The relatively larger number of peak-ring basins on Mercury can then be plausibly explained: for a given impactor population, the higher impact velocity shifts the transition to smaller sizes, where more projectiles are available in the population. The "nested melt-cavity" model of complex crater to multi-ringed basin transitions is primarily linked to natural transitions in the cratering process with increasing size, rather than fundamental properties of the substrate or individual planet; more detailed interplanetary morphometric relationships are influenced by gravity [e.g., *Grieve and Cintala*, 1997] and other parameters such as impact angle [e.g., *Pierazzo and Melosh*, 2000]. The predictions of the model can be further tested and assessed with new observations from terrestrial craters [e.g., *Spray and Thompson*, 2008] and the recent armada of lunar and planetary spacecraft.

References

Bratt, S., S. Solomon, J. Head, and C. Thurber (1985), The deep structure of lunar basins: Implications for basin formation and modification, *J. Geophys. Res.*, *90*, 3049–3064, doi:10.1029/JB090iB04p03049.

Cintala, M., and R. Grieve (1994), The effects of differential scaling of impact melt and crater dimensions on lunar and terrestrial craters: Some brief examples, *Geol. Soc. Am. Spec. Pap.*, *293*, 51–59.

Cintala, M., and R. Grieve (1998), Scaling impact melting and crater dimensions: Implications for the lunar cratering record, *Meteorit. Planet. Sci.*, *33*, 889–912.

Grieve, R., and M. Cintala (1992), An analysis of differential impact melt-crater scaling and implications for the terrestrial cratering record, *Meteoritics*, *27*, 526–538.

Grieve, R., and M. Cintala (1997), Planetary differences in impact melting, *Adv. Space Res.*, *20*, 1551–1560, doi:10.1016/S0273-1177(97)00877-6.

Head, J. (1974), Orientale multi-ringed basin interior and implications for the petrogenesis of lunar highland samples, *Moon*, *11*, 77–99, doi:10.1007/BF01877795.

Head, J. (1977), Origin of outer rings in lunar multi-ringed basins: Evidence from morphology and ring spacing, in *Impact and Explosion Cratering*, edited by D. Roddy et al., pp. 563–573, Pergamon, New York.

Head, J., et al. (1993), Lunar impact basins: New data from the western limb and far side (Orientale and South Pole Aitken basins) from the first Galileo flyby, *J. Geophys. Res.*, *98*, 17,149–17,181, doi:10.1029/93JE01278.

McCauley, J. (1977), Orientale and Caloris, *Phys. Earth Planet. Inter.*, *15*, 220–250, doi:10.1016/0031-9201(77)90033-4.

Melosh, H. (1989), *Impact Cratering: A Geologic Process*, Oxford Univ. Press, London.

Pierazzo, E., and H. Melosh (2000), Melt production in oblique impacts, *Icarus*, *145*, 252–261, doi:10.1006/icar.1999.6332.

Pike, R. (1988), Geomorphology of impact craters on Mercury, in *Mercury*, edited by F. Vilas et al., pp. 165–273, Univ. Ariz. Press, Tucson.

Schultz, P. (1988), Cratering on Mercury: A relook, in *Mercury*, edited by F. Vilas et al., pp. 274–335, Univ. Ariz. Press, Tucson.

Senft, L., and S. Stewart (2009), Dynamic fault weakening and the formation of large impact craters, *Earth Planet. Sci. Lett.*, *287*, 471–482, doi:10.1016/j.epsl.2009.08.033.

Settle, M., and J. Head (1977), Radial variation of lunar crater rim topography, *Icarus*, *31*, 123–135, doi:10.1016/0019-1035(77)90075-6.

Spray, J., and L. Thompson (1995), Friction melt distribution in a multi-ring impact basin, *Nature*, *373*, 130–132, doi:10.1038/373130a0.

Spray, J., and L. Thompson (2008), Constraints on central uplift structure from the Manicouagan impact crater, *Meteorit. Planet. Sci.*, *43*, 2049–2057.

Spudis, P. (1993), *The Geology of Multi-Ring Impact Basins*, 263 pp., Cambridge Univ. Press, Cambridge, U. K.

Weitz, C., J. Head, and C. Pieters (1998), Lunar regional dark mantle deposits: Geologic, multispectral, and modeling studies, *J. Geophys. Res.*, *103*, 22,725–22,759, doi:10.1029/98JE02027.

Wieczorek, M., et al. (2006), The constitution and structure of the lunar interior, *Rev. Mineral. Geochem.*, *60*, 221–364, doi:10.2138/rmg.2006.60.3.

Williams, K., and M. Zuber (1998), Measurements and analysis of lunar basin deposits from Clementine altimetry, *Icarus*, *131*, 107–122, doi:10.1006/icar.1997.5856.

Wood, C., and J. Head (1976), Comparisons of impact basins on Mercury, Mars and the Moon, *Proc. Lunar Sci. Conf.*, *7th*, 3629–3651.

J. W. Head, Department of Geological Sciences, Brown University, Box 1846, 324 Brook St., Providence, RI 02912, USA. (james_head@brown.edu)